Article

Engineering living building materials for enhanced bacterial viability and mechanical properties

Tailor LBM Properties

Cell Viability

Mechanical performance

Biomineralization

Heterotroph   Autotroph

Jishen Qiu, Sherri
Cook, Wil V.
Srubar III, Mija H.
Hubler, Juliana
Artier, Jeffrey C.
Cameron

hubler@colorado.edu (M.H.H.)
jeffrey.c.cameron@colorado.
edu (J.C.C.)

HIGHLIGHTS

Tailoring LBM mechanical
properties via gel/sand
ratio and MICP pathway is
feasible

LBM failure mode varies
with the honeycombed
gel structure and its
biomineralization

Exogenous addition of
desiccation protectant
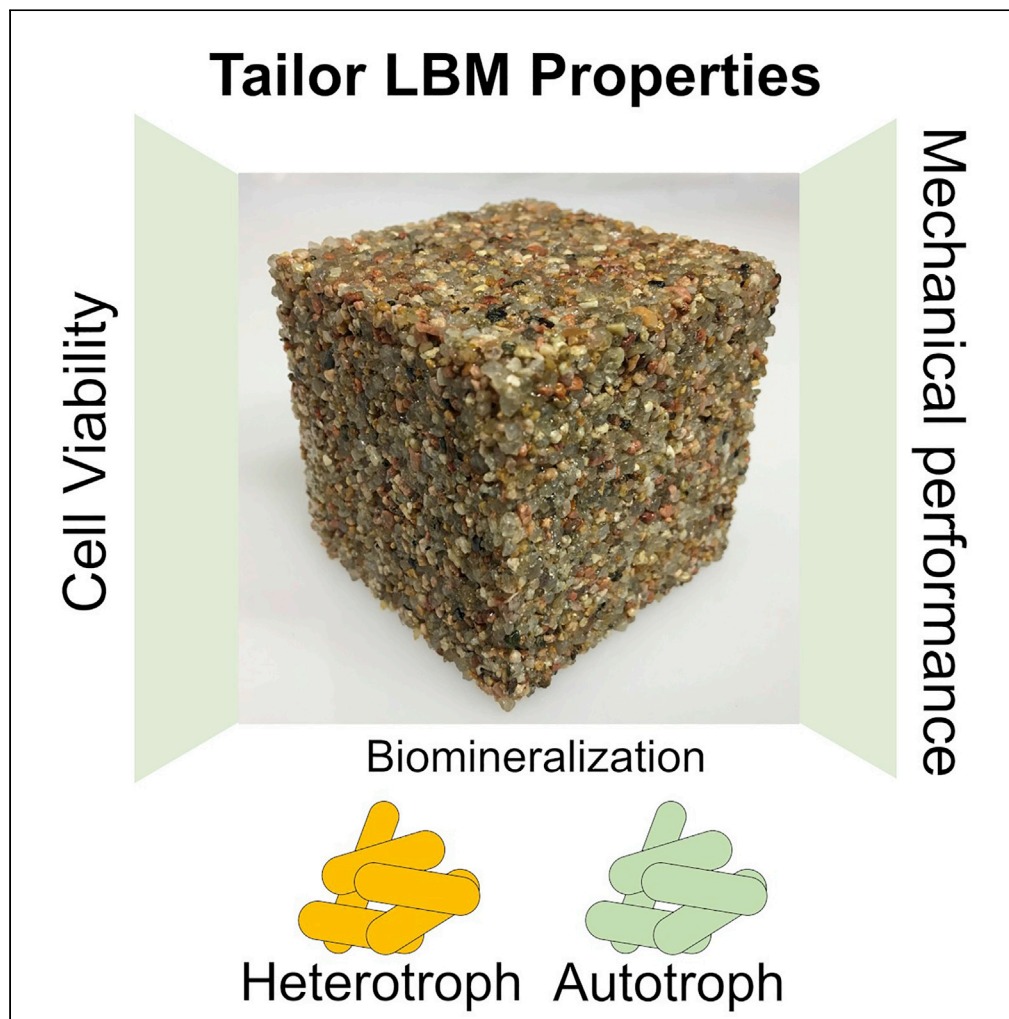trehalose in LBM increases
cell viability

Article

Engineering living building materials for enhanced bacterial viability and mechanical properties

Jishen Qiu,[1,3,4] Sherri Cook,[1] Wil V. Srubar III,[1] Mija H. Hubler,[1,5,*] Juliana Artier,[2,4] and Jeffrey C. Cameron[2,*]

SUMMARY

Living building materials (LBMs) utilize microorganisms to produce construction materials that exhibit mechanical and biological properties. A hydrogel-based LBM containing bacteria capable of microbially induced calcium carbonate precipitation (MICP) was recently developed. Here, LBM design factors, i.e., gel/sand ratio, inclusion of trehalose, and MICP pathways, are evaluated. The results show that non-saturated LBM (gel/sand = 0.13) and gel-saturated LBM (gel/sand = 0.30) underwent distinct failure modes. The inclusion of trehalose maintains bacterial viability under ambient conditions with low relative humidity, without affecting mechanical properties of the LBM. Comparison of biotic and abiotic LBM shows that MICP efficiency in this material is subject to the pathway selected: the LBM with heterotrophic ureolytic *Escherichia coli* demonstrated the most mechanical enhancement from the abiotic controls, compared with either ureolytic or CO_2-concentrating mechanisms from *Synechococcus*. The study shows that tailoring of LBM properties can be accomplished in a manner that considers both LBM microstructure and MICP pathways.

INTRODUCTION

Construction of buildings and infrastructure consumes a lot of resources and contributes to the large-scale production of industrial waste and greenhouse gasses; the production of Portland cement, half of which is used to produce concrete, contributes to 5%-8% of the global CO_2 emission (Benhelal et al., 2013; Shen et al., 2015; Habert et al., 2020). Utilization of renewable building materials and methods of recycling them are critical for environmental sustainability. However, for conventional concrete, chemical reactivity is exhausted with the hydration and hardening of cement; so concrete recycling technology is limited to downcycled utilization of waste concrete as aggregates (Tam, 2009; Shi et al., 2016; Kou and Poon, 2010).

Recently, a novel cement-free living building material (LBM) was developed by the authors, which allows complete material recycling (Heveran et al., 2020). It relies on a bacteria-inoculated "scaffold" made of desiccated gelatin hydrogel to bind sand aggregates. As a load-bearing material, organic hydrogels are generally soft and only suitable for applications like tissue engineering (Sakai et al., 2007; Pok et al., 2013), therefore bacterial cells were added into the gelatin hydrogel to toughen it via microbially induced calcium carbonate precipitation (MICP)—a biotechnology that has been used to enhance soil (Ivanov and Chu, 2008; Van Paassen et al., 2010; Chu et al., 2012) and concrete (De Muynck et al., 2010; Ghosh et al., 2009; Jeong et al., 2017). As desiccated gelatin gels can dissolve again in water under mildly elevated temperature, the solution with bacteria can be recycled and reused to make new LBMs.

In our seminal work, the LBM prototype demonstrated several promising attributes. First, it exhibited high porosity and a density (1,600 kg/m^3) characteristic of lightweight cementitious mortar (Saikia and De Brito, 2012). Low-density materials are advantageous, as they reduce self-weight loading in construction. Second, the MICP enhanced the mechanical properties of the material. Third, the initial bacterial inoculum used to produce the first parent generation of an LBM was used to regenerate up to three child generations without necessitating addition of more biotics (each child generation was made by recycling the hydrogel/bacteria from its parent generation and mixing it with new sands). Nevertheless, practical limitations remain regarding this prototype. The selected bacterial species, i.e., *Synechococcus* sp. PCC 7002, is presumably not as robust as other bacteria because it does not form spores. It only remained viable if the environmental

[1]Department of Civil, Environmental, and Architectural Engineering, University of Colorado Boulder, 1111 Engineering Dr, Boulder, CO 80309, USA

[2]Renewable and Sustainable Energy Institute, University of Colorado Boulder, 4001 Discovery Dr, Boulder, CO 80303, USA

[3]Present address: Department of Civil and Environmental Engineering, The Hong Kong University of Science and Technology, Clear Water Bay, Hong Kong SAR

[4]These authors contributed equally

[5]Lead contact

*Correspondence: hubler@colorado.edu (M.H.H.), jeffrey.c.cameron@colorado.edu (J.C.C.)

https://doi.org/10.1016/j.isci.2021.102083

temperature was low (4°C) and the relative humidity (RH) was high (>50%); yet under the ambient temperature (20°C) and relative humidity (24%), there were no viable cells due to the desiccation of the hydrogel (water loss of about 80%) (Heveran et al., 2020). In addition, the mechanical properties of the LBM were lower than those of conventional cementitious materials used in load-bearing applications (i.e., concrete).

The aim here was to enhance both bacterial viability under ambient conditions (22°C and low RH <50%) and the mechanical properties of the LBMs. Therefore, several important factors that had the potential to improve the less desirable attributes were evaluated. Specifically, a range of gel/sand ratios, which are analogous to the binder/aggregate ratios in traditional concrete design, were evaluated to understand the effect of saturation on the mechanical properties of LBM (Neville, 1996). The term "saturation" here means the inter-particle space within LBM being fully occupied by fresh gel; it does not mean the gel itself being saturated with water. The degree of saturation is important as it may alter the microstructure of the composite, such as inter-aggregate distance and volume fraction of interfacial transition zone (a relatively weak bond between binder and aggregate, Ping and Beaudoin, 1992). To enhance cell viability, especially under ambient conditions, the addition of an exogenous cell desiccation protectant (i.e., trehalose) was evaluated. Trehalose is a simple and well-studied sugar molecule that is used in diverse areas of food and pharmaceutical products to increase chemical stability (Ohtake and Wang, 2011; Luyckx and Baudouin, 2011) and protect cells from desiccation (Welsh and Herbert, 1999). Enhancing viability will be critical for applications such as self-healing concrete and endowing the materials with novel biological properties.

Different MICP pathways can result in different yields and morphologies of the $CaCO_3$ precipitates (Hammes and Verstraete, 2002; Heveran et al., 2019), and it is known that the reinforcing effect to a matrix may increase with the amount and size of micro particles (Wang et al., 2012). So different MICP conditions and bacterial species that direct the MICP pathways involved were also evaluated with the goal of improving the MICP-induced mechanical enhancement. Specifically, three MICP pathways were included. The first was similar to the MICP pathway used in our LBM prototype (Heveran et al., 2020), i.e., the cyanobacteria *Synechococcus* sp. PCC 7002 (referred to as *Synechococcus* in the following discussion) growing and inducing MICP as a result of the CO_2-concentrating mechanism (CCM) (Jansson and Northen, 2010). The other two pathways took advantage of urea degradation, which is known to create a local alkaline environment and induce more MICP (e.g., ureolytic *Sporosarcina pasteurii*, Stocks-Fischer et al., 1999); in this study a bioengineered *Escherichia coli* strain (referred to as *E. coli* in the following discussion) that expresses urease operon from *S. pasteurii* (HB101:pBU11) (Liang et al., 2018; Bachmeier et al., 2002) and the *Synechococcus* sp. PCC 7002, which is also capable of ureolytic activity (Sakamoto et al., 1998), were grown with additional urea to induce MICP. This initial study investigates the engineered ureolytic strain *E. coli* HB101:pBU11, which has the advantage to allow multiple genetic designs capable of greater rational control of $CaCO_3$ precipitation (Liang et al., 2018), leading to variable crystal morphology and nanomechanical properties (Heveran et al., 2019), opening exciting new possibilities for tailoring LBM properties. The three pathways are summarized in Figure 1. Here we show that tailoring these described features had beneficial results in our LBM.

RESULTS AND DISCUSSION

To enhance the mechanical properties of the LBMs, a comparison is made of abiotic versus biotic LBMs made at various gel/sand ratios and using different MICP pathways. Furthermore, it is explored whether supplementation of an exogenous desiccation protectant, trehalose, could increase the viability of the bacteria in the LBMs (see Transparent methods section within the Supplemental Information document for details on experimental procedures).

Mass equilibrium

The non-saturated and saturated LBMs required approximately 7 and 12 days to reach mass equilibrium, respectively (Figure 2). The bulk density of LBMs (~1,600 kg/m^3) was measured to be within the range of lightweight concrete (<1,800 kg/m^3) (Haque et al., 2004). The mass of sand and gel in the LBM at age 0 days and 12 days is given in Table 1.

Compressive and flexural curve of LBMs

Figures 3A and 3B show typical compressive strength-strain curves obtained from the cube tests of non-saturated and saturated specimens, respectively. Figures 3C and 3D show flexural load-crack mouth
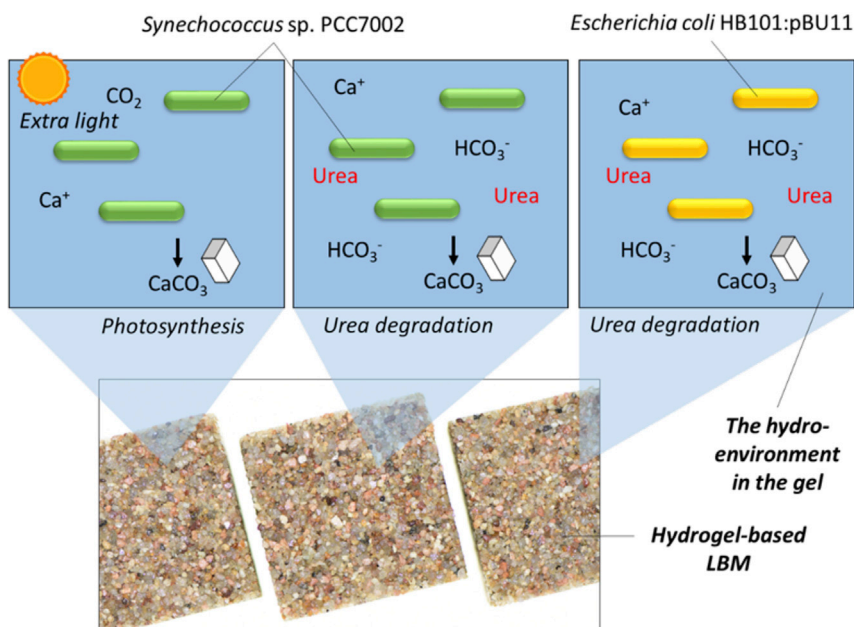
Figure 1. LBMs produced by different MICP pathways in this study

Two different bacteria were used for MICP, the CCM-based cyanobacterium *Synechococcus* sp. PCC 7002 and the heterotrophic *Escherichia coli* expressing urease operon from *S. pasteurii* (HB101:pBU11). Viable cells obtained from LBMs can be used on future material regeneration.

opening displacement (CMOD) curves obtained from the three-point bending tests of the same sample groups (see also Supplemental Information, Figure S1). All the biotic LBMs exhibited similarly shaped compressive and flexural curves. Under compression, the stress increased linearly with strain until the curve approached the peak stress. Compressive strengths of all the measured LBMs are summarized in Table 2.

The non-saturated cubes (gel/sand = 0.13, Figure 3A) and saturated cubes (gel/sand = 0.30, Figure 3B) demonstrated very different post-peak behaviors. More specifically, at gel/sand = 0.13, the stress significantly decreased as the cube fractured. Such a failure mode is comparable to the compressive failure of Portland cement-based mortar. In other words, the specimens dilated horizontally, followed by vertical or X-shaped cracking, which led to failure (Neville, 1996). At gel/sand = 0.30, the cube was able to sustain a tremendous deformation without crumbling, and the stress remained constant. However, the
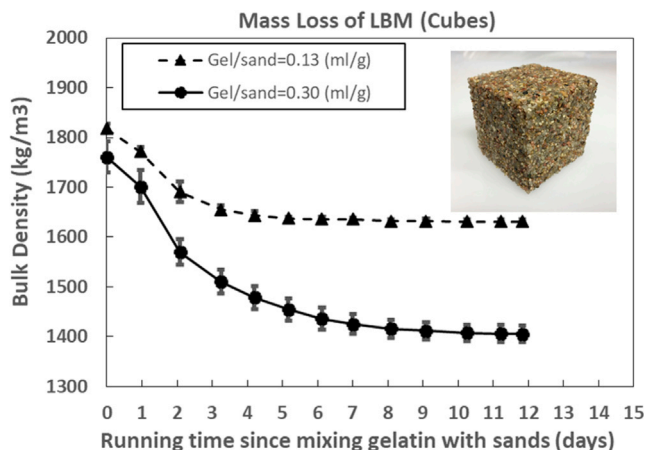
Figure 2. Typical mass loss examples

Non-saturated (gel/sand = 0.13) and saturated LBM (gel/sand = 0.30). Data are represented as mean (n = 3) and +SEM.

Table 1. Mass of sand and gel in LBM before and after desiccation

	Density at 0 day (kg/m^3)		Density at 12 days (kg/m^3)	
Gel/sand ratio (mL g^{-1})	Sand	Initial gel*	Sand	Desiccated gel*
0.13	1,591	227	1,591	43
0.30	1,324	437	1,324	81

compressive strength of saturated cubes was generally lower than that of non-saturated cubes. Under flexure, the load increased linearly with CMOD until the curve approached the peak load. In some cases, multiple peaks were observed, which implies that a flexural crack was arrested multiple times while propagating through the beam depth. After the peak load was reached, the load decreased in a manner similar to fiber-reinforced mortar (Ward et al., 1990), accompanied by widening of the crack, which implies gradual loss of crack-bridging. All the flexural specimens only had one crack at the mid-span. Figure 3 shows that MICP could enhance the mechanical strength of material but did not change its failure modes.

Effect of non-MICP factors on LBM properties

The two biological replicates in all bacterial groups, i.e., Groups 4–9 (Supplemental Information, Table S1), delivered mostly consistent results; for example, compressive strength in 5-1 was 2.59 ± 0.26 MPa and that in 5-2 was 2.53 ± 0.76 MPa (Table 2), indicating the robustness of the MICP methods to manufacture consistent LBMs. Concrete is the most used structural material. The compressive strength of LBMs (~1–4 MPa) is significantly lower than that of conventional concrete (~10–40 MPa), whereas it is only slightly lower than that of lightweight cementitious mortar (Saikia and De Brito, 2012). Its flexural properties are comparable with conventional concrete. The LBM exhibited higher flexural fracture energy (200–1,000 N/m) even when compared with high-strength concretes (e.g., 110–225 N/m for 70- to 80-MPa concrete, Einsfeld and Velasco, 2006, and 140–170 N/m for 40- to 90-MPa concrete, Wu et al., 2001). Hempcrete is a group of green biomaterials that are used as load-bearing elements in houses and low-rise buildings. The compressive strength of LBMs is significantly higher than that of hempcrete (~0.1–1 MPa, Arnaud and Gourlay, 2012). Asphalt concrete is the most used road surface and base course material. The compressive strength of LBMs is comparable to that of asphalt concrete (~3–5 MPa, Gaus et al., 2015). The aforementioned comparisons show the potential of applying LBM in a wide range of light-load-bearing structures.
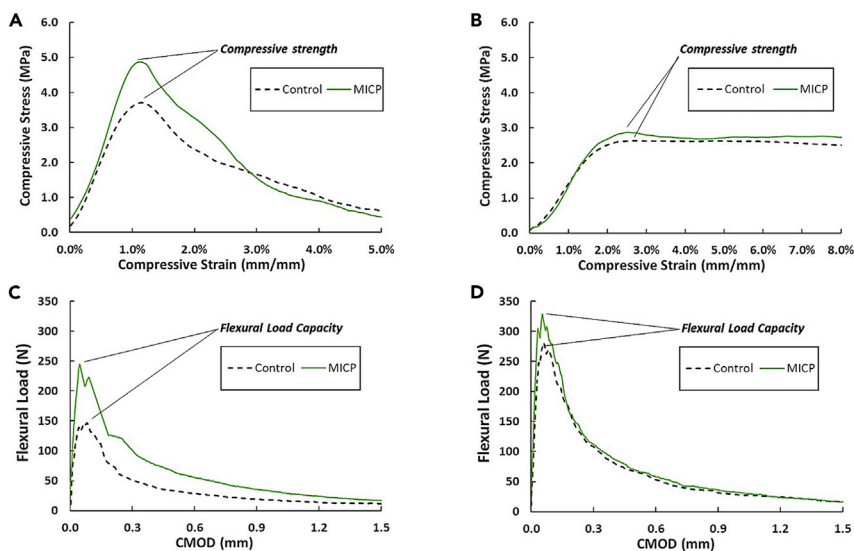
Figure 3. Typical loading curve of LBMs

(A) Compressive curve of non-saturated specimens (gel/sand = 0.13, taken from Group 4 and 4c), (B) compressive curve of saturated specimens (gel/sand = 0.30, taken from Group 5 and 5c), (C) flexural curve of non-saturated specimens (gel/sand = 0.13, taken from Group 4 and 4c), (D) flexural curve of saturated specimens (gel/sand = 0.30, taken from Group 5 and 5c).

Table 2. Summary of LBM mechanical properties

Group[a]	Gel/ sand (mL g^{-1})	Trehalose (mM)	MICP pathways		Compressive strength (MPa) ^	Modulus of rupture (MPa) [b]	Fracture energy (N/m) [b]
			Urea	Bacteria			
1c	0.13	0	No	No	3.71 ± 0.30	1.70 ± 0.15	228 ± 37
2c		20			4.22 ± 0.23	1.92 ± 0.14	227 ± 20
3c		100			3.01 ± 0.18	1.65 ± 0.21	201 ± 14
4c	0.13	200	No	No	3.56 ± 0.51	1.44 ± 0.11	205 ± 77
4-1				Synechococcus	4.82 ± 0.09	2.25 ± 0.21	270 ± 41
4-2				Synechococcus	4.05 ± 0.31	1.61 ± 0.23	159 ± 50
5c	0.30	200	No	No	2.62 ± 0.24	2.48 ± 0.20	252 ± 33
5-1				Synechococcus	2.59 ± 0.26	2.53 ± 0.11	266 ± 18
5-2				Synechococcus	2.53 ± 0.76	2.38 ± 0.42	379 ± 77
6c	0.13	200	Yes	No	2.94 ± 0.25	1.61 ± 0.13	192 ± 18
6-1				Synechococcus	3.77 ± 0.32	1.81 ± 0.22	202 ± 20
6-1				Synechococcus	3.71 ± 0.10	1.89 ± 0.12	256 ± 43
7c	0.30	200	Yes	No	0.92 ± 0.07	2.27 ± 0.36	545 ± 203
7-1				Synechococcus	1.02 ± 0.12	2.25 ± 0.13	735 ± 130
7-2				Synechococcus	1.10 ± 0.04	2.77 ± 0.36	747 ± 246
8c	0.13	200	Yes	No	1.13 ± 0.21	0.96 ± 0.12	437 ± 37
8-1				E. coli	1.49 ± 0.29	1.38 ± 0.18	619 ± 57
8-2				E. coli	2.59 ± 0.22	1.91 ± 0.26	495 ± 82
9c	0.30	200	Yes	No	0.99 ± 0.13	1.66 ± 0.13	675 ± 104
9-1				E. coli	0.93 ± 0.13	1.52 ± 0.16	850 ± 31
9-2				E. coli	1.55 ± 0.01	3.03 ± 0.18	1078 ± 77

[a]For all the biotic groups, the values for each biological replicate (refer to Table 1) are given separately.
[b]The group with the highest value are highlighted.

Most biotic LBMs, except for a few gel/sand = 0.30 groups, showed mechanical enhancement from their controls, indicating that MICP is indeed an effective approach to biomineralize and toughen the hydrogel binders in LBMs. The reduced MICP efficiency at gel/sand = 0.30 specimens is associated with their microstructural failure mode. Several biotic groups exhibit significantly higher mechanical properties compared with our original prototypes in terms of compressive strength (4.82 ± 0.09 MPa of Group 4-1 versus 3.31 ± 0.25 MPa of the prototype), flexural strength (2.77 ± 0.36 MPa of Group 7-2 versus 2.18 ± 0.18 MPa of the prototype), and fracture energy (1,078 ± 77 N/m of Group 9-2 versus 268 ± 31 N/m of the prototype) (Heveran et al., 2020).

The non-saturated LBMs (Group 4/4c, 6/6c, and 8/8c in Table 2) and the saturated ones (Group 5/5c, 7/7c, and 9/9c in Table 2) demonstrated significantly different mechanical properties. The effect of increasing gel content on compressive and flexural strength was opposite: saturated specimens had lower mechanical strength but higher flexural strength and fracture energy. This observation is valid for all conditions tested. The differences are attributable to the different microscopic behaviors of the dehydrated gel under compression and tension, which, respectively, governs the compressive and flexural properties of LBMs. On the other hand, addition of trehalose up to 200 mM only had marginal effects on the mechanical properties of the LBMs (Table 2).

Effect of MICP pathways on LBM properties

Next, the effect of the different MICP pathways on the mechanical properties of the LBMs is measured in *Synechococcus* and *E. coli* at both gel/sand ratios (Figure 4). Similar trends were observed in terms of compressive strength, flexural strength, and fracture energy under all conditions with both strains. The compressive strength and flexural strength decreased at gel/sand = 0.30 in all conditions, whereas the
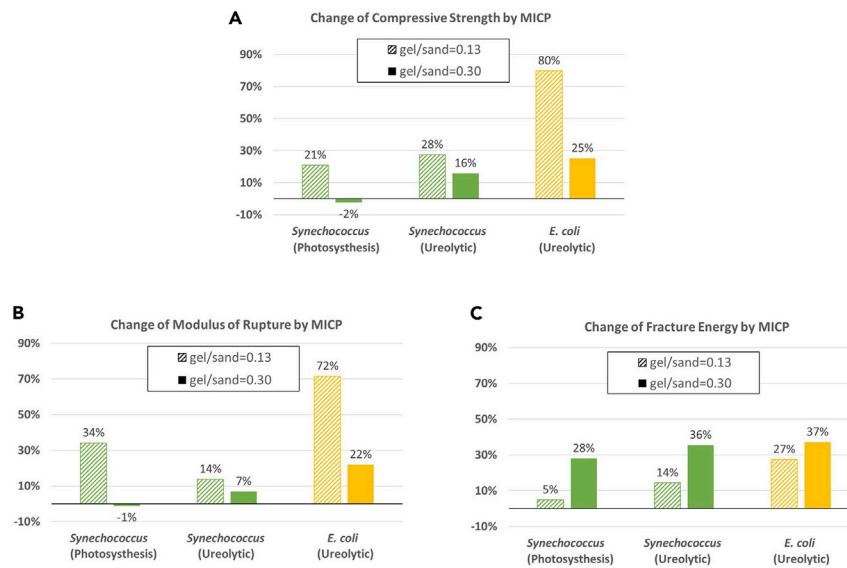
Figure 4. Effect of bacterial metabolism and species on MICP-induced mechanical enhancement of LBMs
(A) Compressive strength, (B) modulus of rupture, (C) fracture energy.

fracture energy was increased, suggesting that gelatin plays a role in preventing crack propagation and energy dissipation.

Microstructures of LBM

Figure 5 shows the typical microstructures of LBMs under a scanning electron microscope. Although the samples here were obtained from failed LBM beams, they were collected from the part that is far away from the central fractured area and not affected by the mechanical loading. Thin-walled honeycomb-like structures, likely formed because of gelatin desiccation and shrinkage, are shown to have bound adjacent sand particles. Although the thin-walled gel is seen in both the non-saturated and saturated specimens, several differences between these formulations are apparent. First, the inter-sand distance in saturated specimens (Figure 5A) is significantly larger than that in non-saturated specimens (Figure 5C), meaning the "wall height" (i.e., the distance between to neighboring sand particles) is larger. Second, the wall thickness in saturated specimens (Figure 5B) is larger than that in non-saturated specimens (Figure 5D). The wall thickness in non-saturated specimens is $6.62 \pm 3.49 \, \mu m$, and in saturated specimens, the wall thickness becomes $16.45 \pm 10.33 \, \mu m$. A histogram of wall thickness shows the distribution of walls thicknesses under both gel/sand conditions (Figure 6).

Rhombohedral $CaCO_3$ precipitates resulting from MICP can be observed in the fractured area of the LBM, embedded within the gelatin (Figure 7). Rhomboid is the typical morphology of MICP crystals (Cuthbert et al., 2012; Qiu et al., 2014). These rhombohedrons were only found in LBMs containing bacteria and not abiotic controls. The diameter of the precipitated crystals (~5–10 μm) is comparable to the wall thickness. It is likely that the crystal inclusion could result in preventing crack propagation through the softer gelatin during mechanical loading, providing a potential mechanism for the mechanical enhancement of fracture energy observed in LBMs containing MICP (Figure 4C).

Several trends regarding the LBM mechanical results have been reported in the previous two sections. For all groups, LBMs demonstrated higher flexural performance, especially fracture energies, which were higher than that of concrete of similar compressive strength grade or comparable to that of concrete of higher compressive strength (e.g., the facture energy of 40-MPa concretes ranges from 100–200 N/m, Wittmann et al., 1990). The mechanical properties of these LBMs are partly attributed to the space between the honeycomb walls; this open space allows for large unhindered deformation like shearing or compression between the adjacent sand particles. Such microstructural failures could absorb significant energy. Supporting evidence to this argument is that the more brittle non-saturated groups are associated with less
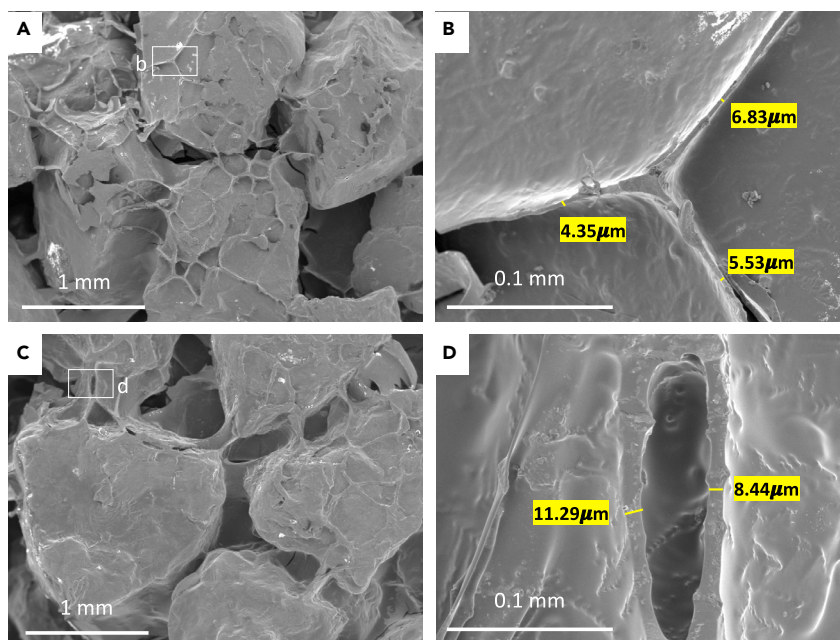
Figure 5. Scanning electron microscopic images of LBMs
(A) Representative microstructures of non-saturated samples (gel/sand = 0.13, Group 4-1), showing that thin-walled honeycomb gel binds sand particles; (B) magnification of (A) and measurement of the wall thickness; (C) representative microstructures of saturated samples (gel/sand = 0.30, Group 5-1), showing thicker gel walls of gel binds sand particles; (D) magnification of (C) and measurement of wall thickness.

space between sand particles than the saturated groups. Although increasing gel content from gel/sand = 0.13 to 0.30 made the LBM less brittle under compressive loading (Figure 3), it reduced its compressive strength. The mechanical results show that at gel/sand = 0.30, MICP is less efficient in enhancing mechanical performance than at gel/sand = 0.13. On the micro-scale, this can be explained with the different micro-structural failure modes (Figure 8). At gel/sand = 0.30, due to the increased wall thickness, the failure tended to happen at the sand-gel interface, or to be more specific, the interface debonded. In this case, the MICP-induced reinforcement of the gel itself was not able to contribute.
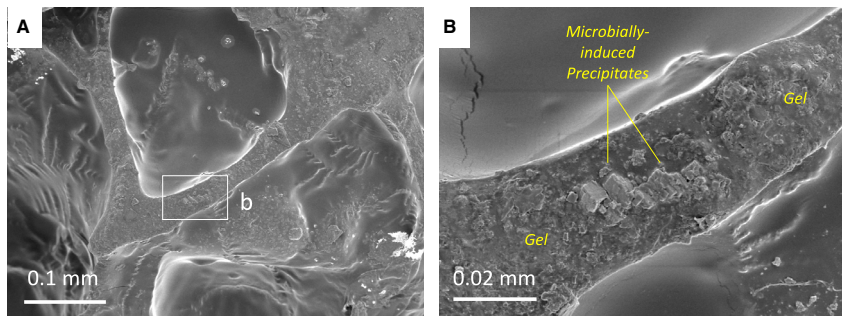
Bacterial viability in LBMs

The results in Figure 9 show that introduction of a desiccation protectant highly improved the bacteria survival in the LBMs cured and stored under ambient conditions (22°C and RH of approximately 15%)
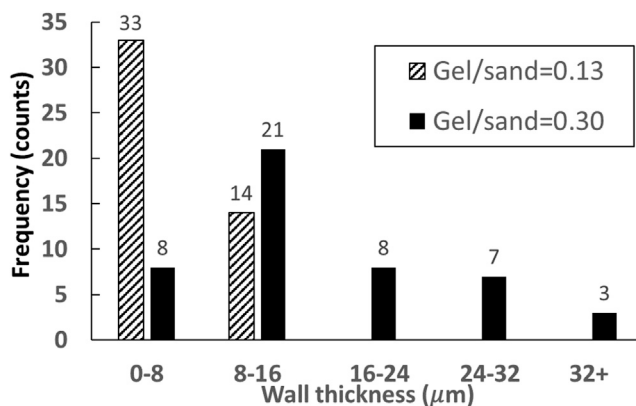
Figure 6. Distribution of wall thickness
Non-saturated samples (gel/sand = 0.13, Group 4) and saturated samples (gel/sand = 0.30, from Group 5).

Figure 7. Microbially induced precipitates found in gel walls in LBMs
Taken from Group 5-1). Panel (A) shows the fractured area of the LBM. Box b is centered on a dehyrated gelatin wall. Panel (B) focuses in on the Box b region. It shows the microbially-induced precipitates within the dehydrated gelatin wall.

compared with our previous study where these LBMs had no viability (Heveran et al., 2020). LBMs with both *E. coli* and *Synechococcus* containing 200 mM trehalose had viable cells after the dehydration period (Figure 9). LBMs with higher gel/sand ratio showed enhanced viability (gel/sand = 0.30 vs. 0.13), possibly due to higher gel (water) content. *Synechococcus* also seemed to tolerate the extreme LBM conditions (i.e., had higher viability) compared with *E. coli*.

Our results present an alternative to the commonly studied ureolytic, spore-forming *S. pasteurii* and accommodate the introduction in LBMs made with organisms sensitive to dry environments. These results were especially important because we were interested in increasing bacterial viability essential for LBM ability of producing recycled child generations (Heveran et al., 2020), particularly when cured under ambient conditions.

Conclusions

Recently a novel LBM made of sand, a hydrogel binder, and bacteria capable of MICP was engineered. The current work experimentally studied the influencing factors on the mechanical performance and bacterial viability in LBMs, including addition of a desiccation protectant (trehalose), different gel/sand ratio, and calcium carbonate precipitation conditions (bacterial species and MICP pathways). The following conclusions can be drawn from the results:

- Increasing the gel/sand ratio from non-saturated (gel/sand = 0.13) to saturated (gel/sand = 0.30) conditions can change the thin-walled honeycomb microstructure of the gel in LBM. Specifically, at gel/sand = 0.30, the wall height and thickness are greater, leading to a higher chance of sand/gel debonding rather than the rupture of the gel wall itself.

- Increasing gel/sand ratio from 0.13 to 0.30 reduces compressive strength but enhances flexural properties of LBM.
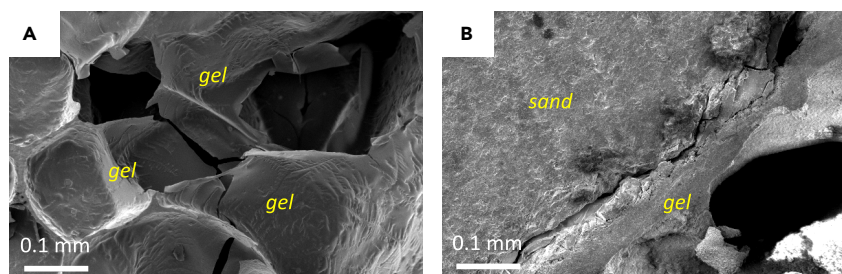
Figure 8. Microstructural failure modes of LBMs
(A) Fracture of the gel walls itself, which was the dominant failure mode of non-saturated specimens (gel/sand = 0.13, Group 4-1); (B) the debonding between the sand particle and the gel, which was commonly seen in saturated specimens (gel/sand = 0.30, Group 5-1).
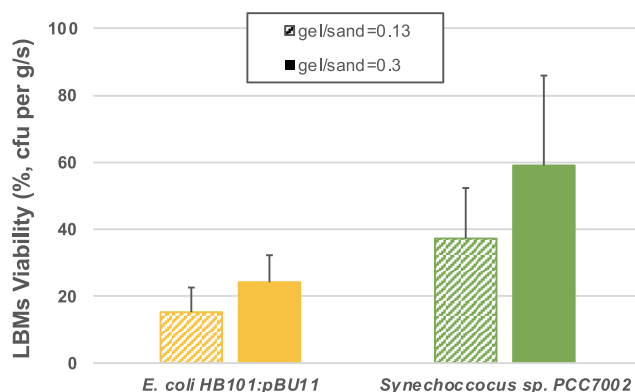
Figure 9. LBM viability

Non-saturated (gel/sand = 0.13) and saturated (gel/sand ratio = 0.3) LBMs with 200 mM trehalose show viable cells after curing for 12 days under ambient conditions (22°C and RH of approximately 15%). The two pathways shown are *E. coli* ureolytic and *Synechococcus* CCM based. Data are represented as mean and +SEM.

- MICP enhances the mechanical properties from all the examined precipitation pathways (*Synechococcus:* CCM pathway, *Synechococcus:* ureolytic, *E. coli* HB101:pBU11: ureolytic). The reinforcing effect of MICP is less efficient at gel/sand = 0.30 because the microstructural failure mode changed from gel failure to sand-gel debonding.

- Addition of a desiccation protectant, such as trehalose, can effectively protect the bacteria from gel dehydration thus maintaining cell viability; meanwhile it does not deteriorate the mechanical properties of LBM up to the gel concentration of 200 mM.

- After the tailoring of the studied factors, LBMs with compressive strength 4.82 ± 0.09 MPa, modulus of rupture 3.03 ± 0.18 MPa, and fracture energy $1,078 \pm 77$ MPa were obtained, which considerably enhanced the prototype LBM (3.31 ± 0.25 MPa, 2.18 ± 0.18 MPa, and 268 ± 31 N/m, respectively), especially considering fracture energy. This study shows that improved mechanical properties can be accomplished by tailoring the manufacturing and processing of LBM.

Limitations of the study

Here we studied two model organisms, the photosynthetic *Synechococcus* sp. PCC 7002 and a genetically engineered version of *E. coli*, capable of MICP and their effect on LBM properties. Yet, further studies will show if the genetic donor of the urease operon, *S. pasteurii,* a natural ureolytic organism, is capable of a similar or higher MICP impact in the proposed LBM. The capability to genetically modify *E. coli*-acquired ureolysis was previously shown to allow biological rational control of calcium carbonate crystals with distinctive morphology and nanomechanical properties. However, if these are capable, or necessary, to tailor and enhance LBM properties will be addressed in future studies.

Resource availability

Lead contact

Further information and requests for resources should be directed to the Lead Contact, Mija H. Hubler (hubler@colorado.edu).

Materials availability

The study did not generate unique reagents.

Data and code availability

All data is available by contacting the lead author. The study did not generate unique code.

METHODS

All methods can be found in the accompanying Transparent methods supplemental file.

SUPPLEMENTAL INFORMATION

ACKNOWLEDGMENTS

AUTHOR CONTRIBUTIONS

J.Q. and J.A. contributed equally to this work. Specific contributions by the authors are stated as follows: study design by J.Q., J.A., S.C., W.V.S., C.C., and M.H.H; data collection and analysis by J.Q. and J.A.; data interpretation by J.Q., J.A., S.C., W.V.S., C.C., and M.H.H.; drafting manuscript: J.Q. and J.A.; all authors approved the final version of this manuscript. J.C.C. acts as corresponding author for his study design and supervision of the biological aspects of the study. M.H.H. acts as corresponding author for her study design and supervision of the mechanics of materials aspects of the study.

DECLARATION OF INTERESTS

W.V.S., S.C., M.H.H., and J.C.C. are inventors on a patent application filed by the University of Colorado on the basis of this work (patent application no. PCT/US2020/020863; filed on 3 April 2020). The authors declare they have no other competing interests.

REFERENCES

Arnaud, L., and Gourlay, E. (2012). Experimental study of parameters influencing mechanical properties of hemp concretes. Construction Building Mater. *28*, 50–56.

Benhelal, E., Zahedi, G., Shamsaei, E., and Bahadori, A. (2013). Global strategies and potentials to curb CO2 emissions in cement industry. J. Clean. Prod. *51*, 142–161.

Chu, J., Stabnikov, V., and Ivanov, V. (2012). Microbially induced calcium carbonate precipitation on surface or in the bulk of soil. Geomicrobiol. J. *29*, 544–549.

Cuthbert, M.O., Riley, M.S., Handley-Sidhu, S., Renshaw, J.C., Tobler, D.J., Phoenix, V.R., and Mackay, R. (2012). Controls on the rate of ureolysis and the morphology of carbonate precipitated by S. Pasteurii biofilms and limits due to bacterial encapsulation. Ecol. Eng. *41*, 32–40.

De Muynck, W., De Belie, N., and Verstraete, W. (2010). Microbial carbonate precipitation in construction materials: a review. Ecol. Eng. *36*, 118–136.

Einsfeld, R.A., and Velasco, M.S. (2006). Fracture parameters for high-performance concrete. Cement Concrete Res. *36*, 576–583.

Gaus, A., Tjaronge, M.W., Ali, N., and Djamaluddin, R. (2015). Compressive strength of asphalt concrete binder course (AC-BC) mixture using buton granular asphalt (BGA). Proced. Eng. *125*, 657–662.

Ghosh, S., Biswas, M., Chattopadhyay, B.D., and Mandal, S. (2009). Microbial activity on the microstructure of bacteria modified mortar. Cement Concrete Compos. *31*, 93–98.

Habert, G., Miller, S.A., John, V.M., Provis, J.L., Favier, A., Horvath, A., and Scrivener, K.L. (2020). Environmental impacts and decarbonization strategies in the cement and concrete industries. Nat. Rev. Earth Environ. *1*, 559–573.

Hammes, F., and Verstraete, W. (2002). Key roles of pH and calcium metabolism in microbial carbonate precipitation. Rev. Environ. Sci. Biotechnol. *1*, 3–7.

Haque, M.N., Al-Khaiat, H., and Kayali, O. (2004). Strength and durability of lightweight concrete. Cement Concrete Compos. *26*, 307–314.

Heveran, C.M., Liang, L., Nagarajan, A., Hubler, M.H., Gill, R., Cameron, J.C., and Srubar, W.V. (2019). Engineered ureolytic microorganisms can tailor the morphology and nanomechanical properties of microbial-precipitated calcium carbonate. Sci. Rep. *9*, 1–13.

Heveran, C.M., Williams, S.L., Qiu, J., Artier, J., Hubler, M.H., Cook, S.M., and Srubar, W.V., III (2020). Biomineralization and successive regeneration of engineered living building materials. Matter *2*, 481–494.

Ivanov, V., and Chu, J. (2008). Applications of microorganisms to geotechnical engineering for bioclogging and biocementation of soil in situ. Rev. Environ. Sci. Biol. Technol. *7*, 139–153.

Jansson, C., and Northen, T. (2010). Calcifying cyanobacteria—the potential of biomineralization for carbon capture and storage. Curr. Opin. Biotechnol. *21*, 365–371.

Jeong, J.H., Jo, Y.S., Park, C.S., Kang, C.H., and So, J.S. (2017). Biocementation of concrete pavements using microbially induced calcite precipitation. J. Microbiol. Biotechnol. *27*, 1331–1335.

Kou, S.C., and Poon, C.S. (2010). Properties of concrete prepared with PVA-impregnated recycled concrete aggregates. Cement Concrete Compos. *32*, 649–654.

Liang, L., Heveran, C., Liu, R., Gill, R.T., Nagarajan, A., Cameron, J.,., and Cook, S.M. (2018). Rational control of calcium carbonate precipitation by engineered Escherichia coli. ACS Synth. Biol. *7*, 2497–2506.

Luyckx, J., and Baudouin, C. (2011). Trehalose: an intriguing disaccharide with potential for medical application in ophthalmology. Clin. Ophthalmol. (Auckland, NZ) *5*, 577.

Neville, A.M. (1996). Properties of Concrete, 4th edition (Wiley).

Ohtake, S., and Wang, Y.J. (2011). Trehalose: current use and future applications. J. Pharm. Sci. *100*, 2020–2053.

Ping, X., and Beaudoin, J.J. (1992). Effects of transition zone microstructure on bond strength

of aggregate-portland cement paste interfaces. Cement Concrete Res. *22*, 23–26.

Pok, S., Myers, J.D., Madihally, S.V., and Jacot, J.G. (2013). A multilayered scaffold of a chitosan and gelatin hydrogel supported by a PCL core for cardiac tissue engineering. Acta Biomater. *9*, 5630–5642.

Qiu, J., Tng, D.Q.S., and Yang, E.H. (2014). Surface treatment of recycled concrete aggregates through microbial carbonate precipitation. Construct. Building Mater. *57*, 144–150.

Saikia, N., and De Brito, J. (2012). Use of plastic waste as aggregate in cement mortar and concrete preparation: a review. Construct. Building Mater. *34*, 385–401.

Sakai, S., Hashimoto, I., and Kawakami, K. (2007). Synthesis of an agarose-gelatin conjugate for use as a tissue engineering scaffold. J. Biosci. Bioeng. *103*, 22–26.

Sakamoto, T., Delgaizo, V.B., and Bryant, D.A. (1998). Growth on urea can trigger death and

peroxidation of the cyanobacterium Synechococcus sp. strain PCC 7002. Appl. Environ. Microbiol. *64*, 2361–2366.

Shen, W., Cao, L., Li, Q., Zhang, W., Wang, G., and Li, C. (2015). Quantifying CO2 emissions from China's cement industry. Renew. Sustain. Energy Rev. *50*, 1004–1012.

Shi, C., Li, Y., Zhang, J., Li, W., Chong, L., and Xie, Z. (2016). Performance enhancement of recycled concrete aggregate–a review. J. Clean. Prod. *112*, 466–472.

Stocks-Fischer, S., Galinat, J.K., and Bang, S.S. (1999). Microbiological precipitation of CaCO3. Soil Biol. Biochem. *31*, 1563–1571.

Tam, V.W. (2009). Comparing the implementation of concrete recycling in the Australian and Japanese construction industries. J. Clean. Prod. *17*, 688–702.

Van Paassen, L.A., Daza, C.M., Staal, M., Sorokin, D.Y., van der Zon, W., and van Loosdrecht, M.C. (2010). Potential soil reinforcement by biological denitrification. Ecol. Eng. *36*, 168–175.

Wang, Q., Hou, R., Cheng, Y., and Fu, J. (2012). Super-tough double-network hydrogels reinforced by covalently compositing with silica-nanoparticles. Soft Matter *8*, 6048–6056.

Ward, R.J., Yamanobe, K., Li, V.C., and Backer, S. (1990). Fracture resistance of acrylic fiber reinforced mortar in shear and flexure. Spec. Publ. *118*, 17–68.

Welsh, D.T., and Herbert, R.A. (1999). Osmotically induced intracellular trehalose, but not glycine betaine accumulation promotes desiccation tolerance in Escherichia coli. FEMS Microbiol. Lett. *174*, 57–63.

Wittmann, F.H., Mihashi, H., and Nomura, N. (1990). Size effect on fracture energy of concrete. Eng. Fracture Mech. *35*, 107–115.

Wu, K.R., Chen, B., Yao, W., and Zhang, D. (2001). Effect of coarse aggregate type on mechanical properties of high-performance concrete. Cement Concrete Res. *31*, 1421–1425.

Supplemental Information

Engineering living building materials

for enhanced bacterial viability

and mechanical properties

Jishen Qiu, Sherri Cook, Wil V. Srubar III, Mija H. Hubler, Juliana Artier, and Jeffrey C. Cameron

Transparent Methods

S. Materials and methods

S.1. Materials

S.1.1. Sand

Sieved natural sand (Colorado, USA) was used as the aggregate. Particle size ranged from 1.18 mm to 2.36 mm. The sand was first rinsed with tap water 5-6 times to remove organics and soluble impurities, then soaked in 4% HCl solution for at least 18 hours to remove possible metallic impurities. To neutralize the acidity, $NaHCO_3$ was added to the saturated sand until it reached a pH 7. In the last step, the sand was oven-dried at 80°C for at least 24 hours. After cooling, the sand was stored at ambient conditions until use.

S.1.2. Gelatin

Commercially available unflavored gelatin powder (Knox) was used as the binding hydrogel scaffold. Gelatin was dissolved in liquid media described below in section S.2.1 at 45°C to form gelatin solutions.

S.1.3. Bacterial Growth

Two different bacterial species were used to induce MICP. *Synechococcus* was maintained in A+ media [Stevens Jr et al., 1973] supplemented with 1 mM sodium thiosulfate and 1% agar. The bacterial cells were inoculated in 25 mL liquid A+ media and grown in a shaker incubator at 180 rpm, 37°C, with ambient CO_2 level, and illumination of approximately 180 µmol photons $m^{-2} s^{-1}$ provided by cool white fluorescent lamps. *E. coli.* HB101:pBU11, previously engineered to express urease using the urease operon from *S. pasteurii* [Jansson and Northen, 2010; Stocks-Fischer et al., 1999], was also used. Prior to MICP, these bacteria were maintained at 37˚C in liquid LB broth containing 50 µM $NiCl_2$ (Ni is a cofactor for urease activity [Christians and Kaltwasser, 1986; Benini et al., 1999; Bachmeier et al., 2002]) and ampicillin 100 µg/mL (for plasmid maintenance).

S.2. Producing LBMs

S.2.1. CaCO₃ precipitation

Synechococcus – **CCM based:** To stimulate MICP through the CCM pathway only, *Synechococcus* prepared in S.1.3 was transferred to a modified A+ medium (supplemented with 25 mM $CaCl_2$ and 25 mM $NaHCO_3$, pH adjusted to 7.6) with a starting inoculum at OD_{730}=0.3 (Group 4 and 5 in **Table S1**). Then it was conditioned in a shaker incubator (180 rpm), 37°C, with ambient CO_2 level, and illumination of approximately 180 μmol (photons) $m^{-2}s^{-1}$ for 24 hours for MICP. OD measurements were performed on a Tecan infinite 200Pro plate reader using Costar 96-well transparent plates.

Synechococcus – **Ureolytic:** To induce MICP using the ureolytic pathway (urea degradation), *Synechococcus* was transferred to the modified A+ medium mentioned above, with slight alterations ($NaNO_3$ was replaced with 50 mM urea, and 5 μM $NiSO_4$ added [Sakamoto and Bryant, 2001]), with starting inoculum at OD_{730}=0.3 (Group 6 and 7 in **Table S1**). Then it was conditioned in a shaker incubator (180 rpm), 37°C, with air supplemented with 3% CO_2, and illumination of approximately 180 μmol (photons) $m^{-2}s^{-1}$ for 4 days.

E. Coli – **Ureolytic:** *E. coli* prepared in S.1.3 was transferred to a urea-$CaCl_2$ medium [Jansson and Northen, 2010; Stocks-Fischer et al., 1999] (supplemented with 5 μM $NiCl_2$ [Bachmeier et al., 2002] and ampicillin 100 μg/mL, pH adjusted to 7.6) with a starting inoculum at OD_{600}=0.2 (Group 8 and 9 in **Table S1**). Then it was conditioned in a shaker incubator (220 rpm), 37°C, with ambient CO_2 level for 4 hours. These conditions were previously shown to successfully promote MICP [Liang et al., 2018].

For all three analyzed conditions (*Synechococcus*- CCM pathway, *Synechococcus*- ureolytic, *E. coli*- ureolytic, **Fig. 1**, and Group 4-9 in **Table S1**), an abiotic control media was prepared (Group 4c-9c in **Table S1**). These media had the same composition and underwent the same treatment (*i.e.,* shaking, temperature, light, level of CO_2 in air). Additionally, abiotic groups (1c-3c in **Table S1**) were prepared with A+ media to study the effect of trehalose concentration (0, 20, 100, 200mM).

Table S1. Summary of the tuned factors for producing LBM specimens, related to **Table 2**

Group[a]	Initial gel/ sand ratio (mL g^{-1})	Trehalose (mM)	MICP pathways		Number of biological replicates[b]	Total number of tested LBMs (cubes/beams)
			Urea	Bacteria		
1c		0			1	3/6
2c	0.13	20	No	No	1	3/6
3c		100			1	3/6
4c	0.13	200	No	No	1	3/6
4				*Synechococcus*	2	6/12
5c	0.30	200	No	No	1	3/6
5				*Synechococcus*	2	6/12
6c	0.13	200	Yes	No	1	3/6
6				*Synechococcus*	2	6/12
7c	0.30	200	Yes	No	1	3/6
7				*Synechococcus*	2	6/12
8c	0.13	200	Yes	No	1	3/6
8				*E. coli*	2	6/12
9c	0.30	200	Yes	No	1	3/6
9				*E. coli*	2	6/12

[a]In this column "c" indicates abiotic control.
[b]For all bacterial groups, two sets of LBMs were made independently.

S.2.2. Preparing gel solution with bacterial precipitates
The prepared biotic media from S.2.1 (Group 4-9), which contained bacterial cells and precipitates, were mixed with gelatin solution containing media components (refer to S.1.2). The abiotic media (Group 1c-9c) were also mixed with this gelation solution. When indicated, trehalose was added at various concentrations (Group 1c to 4c in Table S1). For all the groups, the final gelatin concentration was set at 0.1 g mL^{-1} (10% [w/v]).

S.2.3. Mixing gel and sands to make LBM

Gel solutions from section S.2.2 were gently hand-mixed with dry sand at a gel/sand ratio of 0.13 or 0.30 (Table S1), with approximately 10^7 -10^8 colony forming units (cfus) mL^{-1}. These gel/sand ratios represent distinct degrees of gel saturation: gel/sand=0.13, the sand particles were only surface-moisturized by the gel, so it will be referred to as "non-saturated" in this work; at gel/sand=0.30, the voids between sand particles were fully filled by liquid gel, so it will be referred to as "saturated" in this work. The fresh mixture was left in the mixing bowl in ambient air (22°C and RH of approx. 15%) for 60-80 mins before being cast into cubic molds ($50 \times 50 \times 50$ mm^3) and prismatic molds ($300 \times 25 \times 25$ mm^3). In the next 6-8 hours, the mixture hardened as the gel cooled and physically cross-linked. The specimens were demolded within 24 hours. By the time of demolding, the hydrogel had been able to maintain the structural integrity of LBM despite the relatively higher water content.

S.3. Mechanical characterization

S.3.1. Mass equilibrium

LBM storage and hydrogel desiccation under ambient conditions (22ºC and RH of approx. 15%) led to mass loss of the cubes and prisms, and their mass was monitored daily. The mechanical tests were not carried out until the mass of the LBM reached equilibrium, which was defined as a daily change < 0.2 g (*i.e.,* about 0.1% of the mass recorded at the time of casting). Assuming the mass of sand did not change and all mass reduce resulted from water loss, the mass of gel in the equilibrated LBM was calculated. The effect of water content in hydrogel on the LBM properties were not investigated in the current study.

S.3.2. Uniaxial compression

Uniaxial compressive testing was carried out on the $50 \times 50 \times 50$ mm^3 cubes. The test followed ASTM C109 Standard Test Method for Compressive Strength of Hydraulic Cement Mortars using 2-in. (50-mm) Cube Specimens. An Instron 5869 universal testing machine (UTM) was

used for the compressive testing. The displacement-controlled loading rate was set to be 0.2 mm/s; the recorded load vs. time curve satisfied ASTM C109 (loading rate 900-1800 N/s). The peak load during the test was recorded for the compressive strength calculation. The loading was stopped at 5 mm of displacement for non-saturated specimens and 10 mm for saturated specimens.

S.3.3. Three-point flexure testing of center-notched beams

Three-point flexural tests were carried out on the center-notched $95\times25\times25$ mm^3 small beams; the depth of the central notch was 4 mm. The same Instron UTM was used for the flexural testing. The testing set-up is given in **Figure S1;** two legs of an Epsilon 3542 extensometer were fastened to the bottom of the beam to determine the crack mouth opening displacement (CMOD). A displacement-controlled loading rate at 0.01 mm/s was applied until the CMOD reached 4 mm. The peak load F was used to calculate the modulus of rupture σ (also referred to as flexural strength) in the following equation: $\sigma=1.5FL/(bh^2)$ [ASTM, 2010], where L was the span between two supports (70 mm), b the beam width (25 mm), and h the ligament depth (21 mm). The area under the load-CMOD curve A was used to calculate the fracture energy J in the following equation: $J=A/(bh)$, which is commonly used for quasi-brittle materials [Shah et al., 1995].
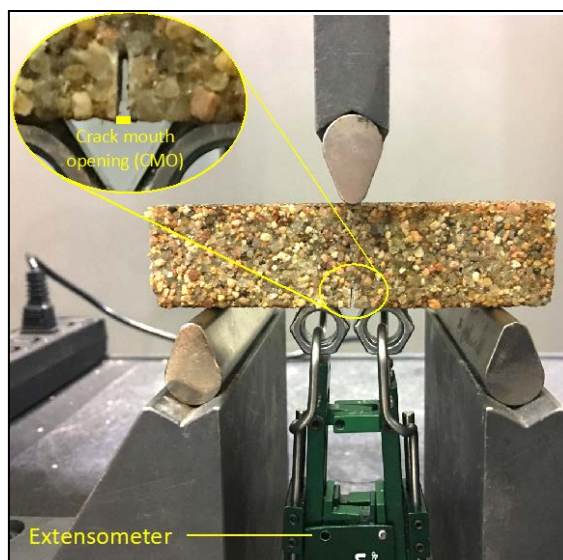
Figure S1. Three-point flexural test setup, related to **Figure 3c** and **3d**.

S.4. Microstructural characterization (SEM)

Tested beams were collected for microstructural characterization. The beams were chipped, and small debris were collected as samples. The samples were sputter coated with a 15-nm coating of gold. The microstructure was observed using a Hitachi SU3500 SEM (accelerating voltage of 5 kV).

S.5. Bacteria viability evaluation

Following mechanical tests, the failed cubes were collected to assess the viability of the bacterial cells in the LBMs. *E. coli* cubes were washed in LB media and *Synechococcus* cubes in A+ media, with 100 mL of media per cube and allowed to shake (250 rpm) until cells were in solution, at 22°C to avoid melting the gelatin from the LBM. The suspension was later centrifuged at 4300 *g* at 22°C for 10 or 20 minutes to collect bacteria cells. The bacterial pellet was resuspended in 1 mL of its respective growth media (section S.2.1) and spread on media solidified with agar (1.5% or 0.5%). Plates with *E. coli* cells were incubated at 37°C overnight. Plates with *Synechococcus* were incubated at 30°C with ambient CO_2 level and illumination of approximately 100 μmol photons $m^{-2}s^{-1}$ until colonies became large enough to count (~72

hours). Colony forming units (cfus) were then counted and the percentage of viable cells was calculated based on the number of cfus in the initial inoculum**.**

Supplementary References

[ASTM, 2010] ASTM, C. (2010). Standard test method for flexural strength of concrete (using simple beam with third-point loading). In *American society for testing and materials* (Vol. 100, pp. 19428-2959).

[Bachmeier et al., 2002] Bachmeier, K. L., Williams, A. E., Warmington, J. R., & Bang, S. S. (2002). Urease activity in microbiologically-induced calcite precipitation. *Journal of biotechnology*, *93*(2), 171-181.

[Benini et al., 1999] Benini, S., Rypniewski, W. R., Wilson, K. S., Miletti, S., Ciurli, S., & Mangani, S. (1999). A new proposal for urease mechanism based on the crystal structures of the native and inhibited enzyme from Bacillus pasteurii: why urea hydrolysis costs two nickels. *Structure*, *7*(2), 205-216.

[Christians and Kaltwasser, 1986] Christians, S., & Kaltwasser, H. (1986). Nickel-content of urease from Bacillus pasteurii. *Archives of microbiology*, *145*(1), 51-55.

[Jansson and Northen, 2010] Jansson, C., & Northen, T. (2010). Calcifying cyanobacteria—the potential of biomineralization for carbon capture and storage. *Current Opinion in Biotechnology*, *21*(3), 365-371.

[Liang et al., 2018] Liang, L., Heveran, C., Liu, R., Gill, R. T., Nagarajan, A., Cameron, J., ... & Cook, S. M. (2018). Rational Control of Calcium Carbonate Precipitation by Engineered Escherichia coli. *ACS synthetic biology*, *7*(11), 2497-2506.

[Sakamoto and Bryant, 2001] Sakamoto, T., & Bryant, D. A. (2001). Requirement of nickel as an essential micronutrient for the utilization of urea in the marine cyanobacterium Synechococcus sp. PCC 7002. *Microbes and Environments*, *16*(3), 177-184.

[Shah et al., 1995] Shah, S. P., Swartz, S. E., & Ouyang, C. (1995). <u>Fracture mechanics of concrete: applications of fracture mechanics to concrete, rock and other quasi-brittle materials</u>. John Wiley & Sons.

[Stevens Jr et al., 1973] Stevens Jr, S. E., Patterson, C. P., & Myers, J. (1973). The Production of Hydrogen Peroxide by Blue-Green Algae: A Survey 1. *Journal of Phycology*, *9*(4), 427-430.

[Stocks-Fischer et al., 1999] Stocks-Fischer, S., Galinat, J. K., & Bang, S. S. (1999). Microbiological precipitation of CaCO3. *Soil Biology and Biochemistry*, *31*(11), 1563-1571.